

ERROR ESTIMATION FOR THE DKMQ24 SHELL ELEMENT USING VARIOUS RECOVERY METHODS

Irwan Katili^{1*}, Imam Jauhari Maknun¹, Elly Tjahjono¹, Irene Alisjahbana¹

¹*Department of Civil Engineering, Faculty of Engineering, Universitas Indonesia, Kampus UI Depok, Depok 16424, Indonesia*

(Received: January 2017 / Revised: May 2017 / Accepted: November 2017)

ABSTRACT

This paper presents an application of the DKMQ24 element for error estimation using error estimator Z^2 and various recovery methods such as Averaging (AVR), Projection (PROJ) and Superconvergent Patch Recovery (SPR). The stresses found by using these recovery methods were compared to the reference solution. It was found that the AVR and SPR methods gave better results than PROJ method.

Keywords: Averaging; DKMQ24; Error estimation; Shell element; Projection; SPR

1. INTRODUCTION

The rapid advancement of technology in computation and material for civil engineering has encouraged construction designers to create more sophisticated and futuristic building. When dealing with complex structures, it is difficult to determine the deformation that occurs, as there is no exact solution. To understand such a structure, modeling of the structure, it is necessary to model the structure using numerical simulation. The Finite Element Method (FEM) is a numerical method which can be used to solve various problems in structures, soil mechanics, fluids, etc. More specially, FEM is an approximation method where the exact solution is estimated using a repetitive discretization process by increasing the element number or refining the element size. A discretization strategy must be taken in each mesh refinement process in order to obtain a solution that is as close as possible to the exact one.

Errors in FEM are unavoidable; these may be caused by inappropriate models and numerical integration, inaccuracy of the numerical solution, or rounding errors in the numerical process. The errors produced in FEM are difficult to determine since complex problems usually have no exact solution. Therefore, an error estimator is developed to get a solution as close as possible to the exact one.

A simple error estimator, called error estimator ' Z^2 ', was proposed by Zienkiewicz and Zhu (1987) and can be applied easily in FEM programs. In addition, they also presented recovery methods, called Averaging (AVR) and Projection (PROJ). The application of error estimator Z^2 in plate bending problems was then presented by Zienkiewicz and Zhu in 1989. Triangular elements with uniform and adaptive meshes were used and it was found that error estimator Z^2 is very effective. Zienkiewicz and Zhu (1992a, 1992b, 1992c) also introduced the first superconvergent method, called the Superconvergent Patch Recovery (SPR) method, where the element nodal forces are recovered by the least square fit. Yunus et al. (1990) demonstrated the

*Corresponding author's email: irwan.katili@eng.ui.ac.id, Tel: +62-21-7270029, Fax: +62-21-7270028
Permalink/DOI: <https://doi.org/10.14716/ijtech.v8i6.699>

effectiveness of the AVG and PROJ methods by analyzing plate and shell problems. However, these two methods are less precise than the SPR method. Another superconvergent method called Recovery by Equilibrium in Patches (REP), was proposed by Boroomand and Zienkiewicz (1997a, 1997b) and Boroomand et al. (2004). This method uses the equilibrium of the solution to produce recovered internal forces. A recovery method called the Recovery of Stresses by Compatibility in Patches (RCP) was proposed by Ubertini (2004). Other recovery methods have also been presented by different authors, including Zhang and Naga (2004) and Payen and Bathe (2011, 2012).

In FEM, the use of many different types of elements have been proposed by different authors. DKMT and DKMQ elements, which are able to analyze thick to thin plate bending problems have been proposed by Katili (1993a, 1993b). DKMT and DKMQ elements are free of shear locking in thin plate problems and give good results for thin to thick plate problems. The formulation of DKMQ and DKMT plate elements is based on the Reissner–Mindlin hypothesis (Mindlin, 1951; Reissner, 1972) which only requires C^0 continuity. Batoz and Katili (1992) proposed another triangular element called DST-BK, based on the free formulation method.

The application of DKMQ element in composite structures has been presented by (Katili et al., 2015). Another application of DKMQ for buckling analysis is presented in (Wong et al., 2017) and for stochastic finite element analysis in (Mahjudin et al., 2016)

Moreover, the development of the DKMT element for error estimation in composite plate structures has been presented by Maknun et al. (2015). Meanwhile, Katili et al. (2015) have presented the development of the DKMQ plate element to the DKMQ24 shell element using the Naghdi/Mindlin/Reissner shell theory, which takes into account warping effects and coupling bending-membrane energy effects. This element passed the patch tests for membrane, bending and shear problems. It also successfully passed benchmark tests for the cases of thick and thin shells without shear locking. The numerical results obtained with DKMQ24 converge toward the reference solution. Furthermore, Maknun et al. (2016) have compared the application of the DKMQ24 element for twist thin-walled beams to the Vlassov theory based on simplification (Hamdouni et al., 2016). A new development of the DKMQ20 shell element with five degrees of freedom has been presented by Irpani et al. (2017).

In this paper, the application of the DKMQ24 element for error estimation using error estimator Z^2 and various recovery methods such as AVR, PROJ and SPR will be analyzed. The stresses found by using these recovery methods will be compared to the reference solution.

2. FORMULATION OF DKMQ24 ELEMENT

The DKMQ24 element that will be used in this study for the numerical simulations is developed from the DKMQ plate element using the Naghdi/Mindlin/Reissner shell theory. Therefore, the warping and coupling bending-membrane energy effects are taken into account in the formulation of the element. The reader may find more details about this in Katili et al. (2015). The finite element formulation of DKMQ24 is based on the Naghdi shell model (see Katili et al. 2015). Introducing the interpolation functions $N_i(\xi, \eta)$, the position vectors \underline{x}_q of a point q of the shell can be written as:

$$\underline{x}_q(\xi, \eta, z) = \sum_{i=1}^4 N_i(\xi, \eta) \underline{x}_i + z \sum_{i=1}^4 N_i(\xi, \eta) \underline{n}_i \quad (1)$$

The displacement of \underline{u}_q is given by:

$$\underline{u}_q(\xi, \eta, z) = \langle u_p(\xi, \eta) \rangle + z \underline{\beta}(\xi, \eta) \quad \text{with} \quad \underline{\beta} \cdot \underline{n} = 0 \quad (2)$$

where $\underline{\beta}(\xi, \eta)$ represents the rotation vector. Moreover, we have:

$$\underline{u}_q(\xi, \eta, z) = \sum_{i=1}^4 N_i(\xi, \eta) \begin{Bmatrix} U_i \\ V_i \\ W_i \end{Bmatrix} + z \left(\sum_{i=1}^4 N_i [RN]_i \begin{Bmatrix} \theta_{Xi} \\ \theta_{Yi} \\ \theta_{Zi} \end{Bmatrix} + \sum_{k=5}^8 P_k \{t_{sk}\} \Delta\beta_{sk} \right) \quad (3)$$

where N_i are linear functions of interpolation and P_k are incomplete quadratic functions (see Table 1).

Table 1 Linear interpolation functions N_i and quadratic functions P_k

$N_1 = \frac{1}{4}(1-\xi)(1-\eta)$	$P_5 = \frac{1}{2}(1-\xi^2)(1-\eta)$
$N_2 = \frac{1}{4}(1+\xi)(1-\eta)$	$P_6 = \frac{1}{2}(1+\xi)(1-\eta^2)$
$N_3 = \frac{1}{4}(1+\xi)(1+\eta)$	$P_7 = \frac{1}{2}(1-\xi^2)(1+\eta)$
$N_4 = \frac{1}{4}(1-\xi)(1+\eta)$	$P_8 = \frac{1}{2}(1-\xi)(1-\eta^2)$

The vector $\underline{t}_{s_k} = \underline{x}_{ji} / L_k$ ($k = 5, 6, 7, 8$) is a unit vector tangential on the side of the element. Moreover, $\Delta\beta_{s_k}$ ($k = 5, 6, 7, 8$) is a temporary degree of freedom in the middle side of the element and will be eliminated using the discrete Kirchhoff-Mindlin method (Katili et al., 2015). Figure 1 show the nodal degrees of freedom for the DKMQ24 element.

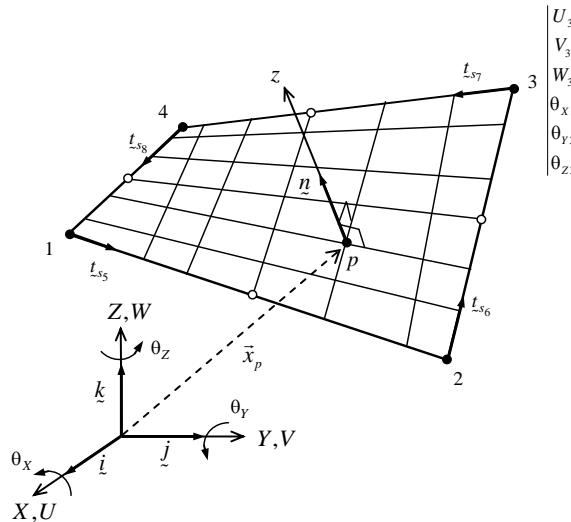


Figure 1 Degrees of freedom DKMQ24 element

3. RECOVERY METHODS

While the FEM solution has been known to provide continuity in displacement at nodal points, it yields discontinuity and inaccuracy problems when used to calculate internal forces at the joined sides of the boundary elements. The nature of the FEM solution, which means that

internal forces are calculated using the derivation of the displacement function, has created such a problem. To obtain continuity in the internal force, there are several methods that can be used. These are outlined below:

3.1. Averaging Method

The recovery of internal forces is taken from the average value of the finite element results for each element:

$$\{N^*\}_i = \frac{1}{m} \sum_i^m \{N^h\}_i \quad ; \quad \{M^*\}_i = \frac{1}{m} \sum_i^m \{M^h\}_i \quad ; \quad \{T^*\}_i = \frac{1}{m} \sum_i^m \{T^h\}_i \quad (4)$$

where $\{N^*\}_i$, $\{M^*\}_i$ and $\{T^*\}_i$ are the recovered membrane, moment and shear forces, while, $\{N^h\}_i$, $\{M^h\}_i$ and $\{T^h\}_i$ are the finite element results of the membrane, moment and shear forces at node i , and m is the number of elements connected at node i .

3.2. Projection Method

The recovered bending moments M^* is assumed as:

$$M_x^* = \langle N \rangle \{M_{x_n}^*\} \quad (5)$$

where N is the interpolation function (see Table 1). Using the weight residual method proposed by Zienkiewicz and Zhu (1987) gives:

$$\int_A \{N\} (M_x^* - M_x^h) dA = 0 \quad (6)$$

Substituting (5) into (6), we have:

$$\int_A \{N\} \langle N \rangle dA M_{x_n}^* = \int_A \{N\} M_x^h dA \quad (7)$$

With a little simplification, we obtain:

$$\{M_{x_n}^*\} = [P]^{-1} \int_A \{N\} M_x^h dA \quad \text{with} \quad [P] = \int_A \{N\} \langle N \rangle dA \quad (8)$$

3.3. Superconvergent Patch Recovery

The SPR method is relatively simple and may easily be used in finite element analysis. The aim is to recover the finite element result with the least square fit method analogy. The recovered moment (or membrane or shear) force M^* is assumed as:

$$\begin{aligned} M_x^* &= \langle P(\xi, \eta) \rangle \{a_n\} \\ \langle P(\xi, \eta) \rangle &= \langle 1 \quad \xi \quad \eta \quad \xi^2 \quad \xi\eta \quad \eta^2 \quad \xi^2\eta \quad \xi\eta^2 \rangle \\ \{a_n\} &= \langle a_n \rangle^T = \langle a_1 \quad a_2 \quad a_3 \quad a_4 \quad a_5 \quad a_6 \quad a_7 \quad a_8 \rangle^T \end{aligned} \quad (9)$$

where $\langle P \rangle$ is the polynomial expansion function in parametric local coordinate system (ξ, η) in the local patch (see Figure 2). The unknown parameter $\{a_n\}$ is solved by minimizing the following function

$$\Phi = \sum_{k=1}^n \left[M_x^h(\xi_k, \eta_k) - \langle P(\xi_k, \eta_k) \rangle \{a_n\} \right]^2 \quad (10)$$

where (ξ_k, η_k) is a Gauss point in the local patch coordinate system, n is the Gauss point number in the patch, and $M_x^h(\xi_k, \eta_k)$ is the finite element result. The minimization yields:

$$\sum_{k=1}^n \langle P(\xi_k, \eta_k) \rangle^T \langle P(\xi_k, \eta_k) \rangle \{a_n\} = \sum_{k=1}^n \langle P(\xi_k, \eta_k) \rangle^T M_x^h(\xi_k, \eta_k) \quad (11)$$

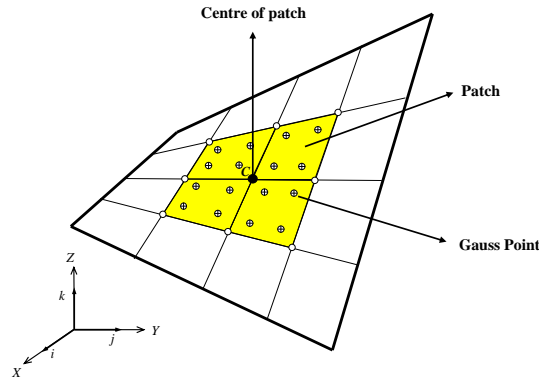


Figure 2 Nodal based Patch

Finally the unknown parameter $\{a_n\}$ is:

$$\begin{aligned} \{a_n\} &= [A]^{-1} \{b_n\} \\ \text{with } [A] &= \sum_{k=1}^n \langle P_k \rangle^T \langle P_k \rangle \quad \text{and} \quad \{b_n\} = \sum_{k=1}^n \langle P_k \rangle^T M_x^h(\xi_k, \eta_k) \end{aligned} \quad (12)$$

The recovered internal forces can be calculated by using Equation 8.

4. ERROR ESTIMATOR Z^2

Since the calculation will not stop until the element size is close to zero, an effective condition is required as a criterion to terminate the discretization process. The factor for the relative error ϕ^* of a structure using the recovery method is shown in Equation 13. The error indicator represents the value that is used as a criterion to terminate the refinement process. Usually, $\phi^* = 5\%$ is taken as a limit. Following Zienkiewicz and Zhu (1987), the factor for the relative error is calculated as:

$$\phi^* = \frac{\|e^*\|}{\|u^*\|} \times 100\% \quad (13)$$

where

$$\begin{aligned} \|e^*\|^2 &= \sum_{i=1}^m \|e_i^*\|^2 \\ \|e_i^*\|^2 &= \int_A (\langle N^* \rangle - \langle N^h \rangle) [H_m]^{-1} (\{N^*\} - \{N^h\}) dA + \int_A (\langle M^* \rangle - \langle M^h \rangle) [H_b]^{-1} (\{M^*\} - \{M^h\}) dA \\ &\quad + \int_A (\langle T^* \rangle - \langle T^h \rangle) [H_s]^{-1} (\{T^*\} - \{T^h\}) dA \end{aligned}$$

and

$$\|u^*\|^2 = \sum_{i=1}^m \|u_i^*\|^2$$

$$\|u_i^*\|^2 = \int_A \langle N^* \rangle [H_m]^{-1} \{N^*\} dA + \int_A \langle M^* \rangle [H_b]^{-1} \{M^*\} dA + \int_A \langle T^* \rangle [H_s]^{-1} \{T^*\} dA$$

5. NUMERICAL RESULTS AND DISCUSSION

In this section, the results of the error estimation using various recovery methods and the error estimator Z^2 are presented. A relative error factor of $\phi^* = 5\%$ was used as a limit to terminate the refinement process. Mesh $N \times N = 4 \times 4, 8 \times 8, 16 \times 16$ and 32×32 were employed.

5.1. Scordelis–Lo Roof Problem

Owing to its symmetry, only a quarter of the structure was analyzed. In this example, the membrane effect was more dominant. The boundary conditions were $U = W = \theta_Y = 0$ on the side AD , while the symmetry conditions were $U = \theta_Y = \theta_Z = 0$ on the side CD and $V = \theta_X = \theta_Z = 0$ on the side CB .

- $L = 6\text{ m};$
- $R = 3\text{ m};$
- $h = 0.03\text{ m};$
- $\phi = 40^\circ;$
- $E = 3 \times 10^{10}\text{ Pa};$
- $\nu = 0;$
- $F_z = -0,625 \times 10^4\text{ Pa}$

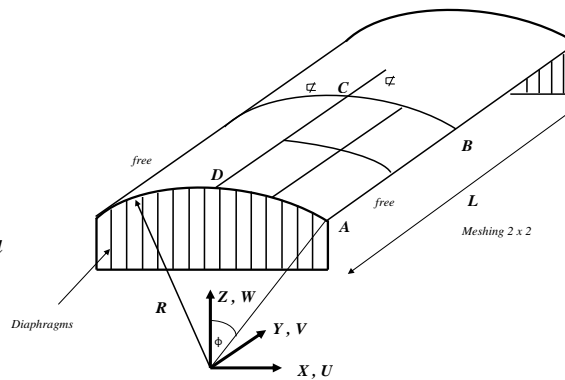


Figure 3 Scordelis–Lo roof problem

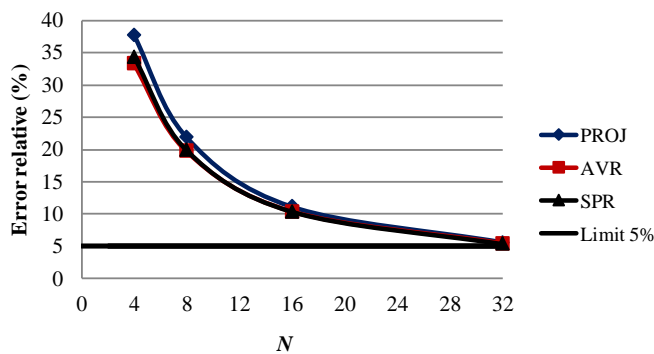


Figure 4 Relative error Indicator ϕ^* Scordelis–Lo roof problem

The results of the numerical test are presented in Figures 4 and 5 and Table 2. For the 32×32 mesh, as can be seen in Figure 4, the relative error indicator ϕ^* results are close to the limit of 5%. It was observed that all recovery methods gave the similar relative error factors ϕ^* for this case. However, it can also be seen that the AVR and SPR methods converged faster than the PROJ method.

Figure 5 and Table 2 present the effort membrane in the Y direction at point B (N_{YB}) and the effort moment in the X direction at point C (M_{XC}). The results from Scordelis and Lo (1969)

were used as the reference solution. For N_{YB} , the convergence of the AVR and SPR methods was faster than that of the PROJ method. Meanwhile for M_{XC} , it was observed that all recovery methods gave similar results. However, it can be observed that the AVR and SPR methods gave better results than the PROJ method in coarse mesh. The details of the results are displayed in Table 2.

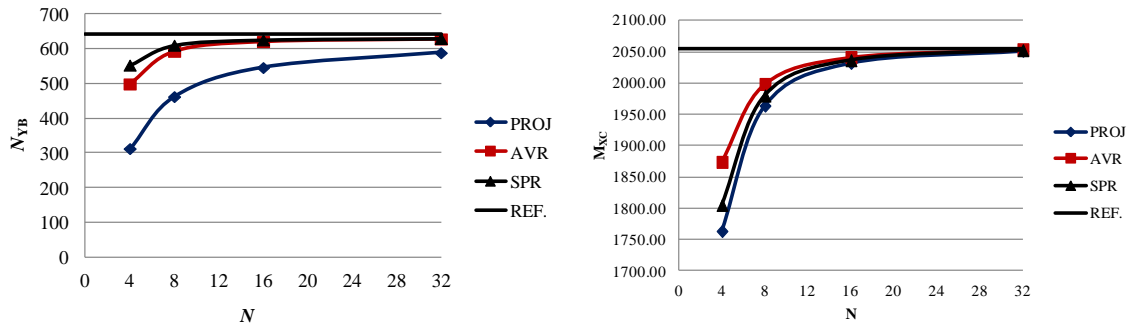


Figure 5 N_{YB} and M_{XC} Scordelis–Lo roof problem

Table 2 N_{YB} and M_{XC} Scordelis–Lo roof problem

N	N_{YB}			M_{XC}		
	AVR	PROJ	SPR	AVR	PROJ	SPR
4	498.430	312.020	552.820	1873.80	1763.30	1805.00
8	592.680	461.930	610.200	1998.30	1963.70	1979.80
16	620.750	545.710	625.610	2041.30	2032.00	2036.30
32	628.280	588.400	629.550	2053.80	2051.30	2052.30
REF.		641			2056	

5.2. Pinched Cylindrical Shell with End Diaphragms

The shell presented in Figure 6 is a pinched cylinder with two concentrated loads situated in opposite directions. At either end, there is a rigid diaphragm. Due to its symmetry, only 1/8 of the structure was analyzed. The boundary condition was $U = W = \theta_Y = 0$ on the side AD ; meanwhile, the symmetry conditions were $W = \theta_Y = \theta_X = 0$ on the side AB , $V = \theta_X = \theta_Z = 0$ on the side BC , and $U = \theta_Y = \theta_Z = 0$ on the side CD .

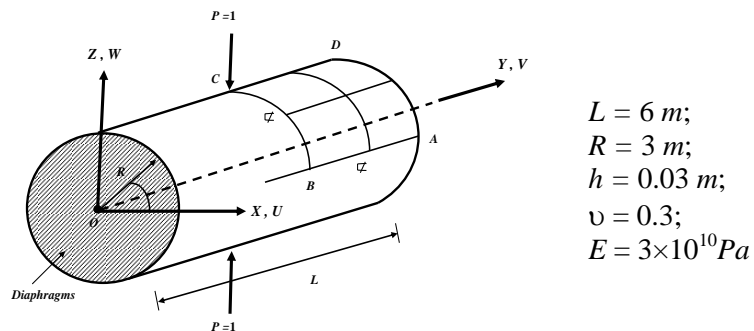


Figure 6 Pinched cylindrical shell

The relative error indicator ϕ^* is presented in Figure 7a. Once again, it can be observed that the AVR and SPR methods converged faster than the PROJ method. In this case, the PROJ method gave a relative error indicator of 13.34% for the 32×32 mesh. Meanwhile, the AVR and SPR methods gave a relative error indicator equal to 7.5% by using similar meshes. Figure 8b

presents the effort moment along the side DC . The results from Lindberg et al. (1969) were used as the reference solution. It can be observed that the convergence of the AVR and SPR methods was faster than that of the PROJ method, and the results given by these two methods were closer to the reference solution.

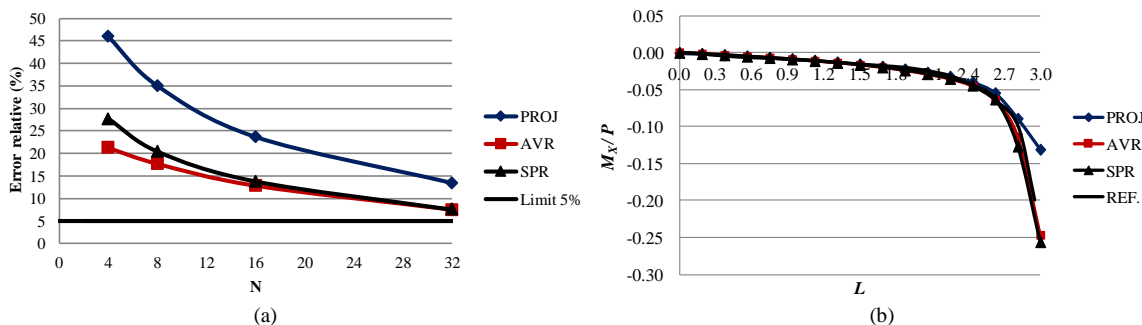


Figure 7 Relative error indicator ϕ^* and M_x along side DC of pinched cylindrical shell

6. CONCLUSION

The application of the DKMQ24 element for error estimation in shell structure by using various recovery methods has been presented. The Scordelis–Lo roof and pinched cylindrical shell have also been analyzed. Regarding the relative error indicator ϕ^* and internal forces after recoveries, it was found that AVG and SPR methods give better results than the PROJ method. This phenomenon can be seen in the N_{YB} for the Scordelis–Lo roof problem and the relative error indicator ϕ^* for the pinched cylindrical shell. For the Scordelis–Lo roof problem, the PROJ method gave $N_{YB} = 588.400$ using 32×32 mesh, while the reference solution was equal to 641 (it produced 8% more errors than the reference solution). For the pinched cylindrical shell, the PROJ method gave a relative error indicator of 13.34% for 32×32 mesh. Meanwhile, the AVR and SPR methods produced a relative error indicator equal to 7.5% by using similar meshes.

7. ACKNOWLEDGEMENT

The financial support from the Indonesian Ministry of Research, Technology and Higher Education (KEMENRISTEKDIKTI) and Universitas Indonesia through the Hibah Publikasi Internasional Terindeks untuk Tugas Akhir Mahasiswa (Hibah PITTA) No. 786/UN2.R3.1/HKP.05.00/2017 are gratefully acknowledged.

8. REFERENCES

Batoz, J.-L., Katili I., 1992. On a Simple Triangular Reissner/Mindlin Plate Element based on Incompatible Modes and Discrete constraints. *International Journal for Numerical Methods in Engineering*, Volume 35, pp. 1603–1632

Boroomand, B., Zienkiewicz, O.C., 1997. Recovery by Equilibrium in Patches (REP). *International Journal for Numerical Methods in Engineering*, Volume 40, pp. 137–164

Boroomand, B., Zienkiewicz, O.C., 1997. An Improved REP Recovery and the Effectivity Robustness Test. *International Journal for Numerical Methods in Engineering*, Volume 40, pp. 3247–3277

Boroomand, B., Ghaffarian, M., Zienkiewicz, O.C., 2004. On Application of Two Superconvergent Recovery Procedures to Plate Problems. *International Journal for Numerical Methods in Engineering*, Volume 61, pp. 1644–1673

- Hamdouni, A., Katili, I., Maknun, I.J., Millet, O., 2013. Analytical and Experimental Analysis of an Asymptotic Thin-walled Beam Model. *European Journal of Environmental and Civil Engineering*, Volume 17(1), pp. 1–18
- Irpanni, H., Katili I., Maknun I.J., 2017. Development DKMQ Shell Element with Five Degrees of Freedom per Nodal. *International Journal of Mechanical Engineering and Robotics Research*, Volume 6, pp. 248–252
- Katili, I., 1993. A New Discrete Kirchhoff-Mindlin Element based on Mindlin-Reissner Plate Theory and Assumed Shear Strain Fields- Part I: an Extended DKT Element for Thick-plate Bending Analysis. *International Journal for Numerical Methods in Engineering*, Volume 36, pp. 1859–1883
- Katili, I., 1993. A New Discrete Kirchhoff-Mindlin Element based on Mindlin-Reissner Plate Theory and Assumed Shear Strain Fields- Part II: an Extended DKQ Element for Thick Plate Bending Analysis. *International Journal for Numerical Methods in Engineering*, Volume 36, pp. 1885–1908
- Katili, I., Maknun, I.J., Millet, O., Hamdouni, A., 2015. Application of DKMQ Element for Composite Plate Bending Structures. *Composite Structures*, Volume 132, pp. 166–174
- Katili, I., Batoz, J.L., Maknun, I.J., Hamdouni, A., Millet, O., 2015. The Development of DKMQ Plate Bending Element for Thick to Thin Shell Analysis based on Naghdi/Reissner/Mindlin Shell Theory. *Finite Elements in Analysis and Design*, Volume 100, pp. 12–27
- Katili, I., 2017. Unified and Integrated Approach in a New Timoshenko Beam Element. *European Journal of Computational Mechanics*, Volume 26, pp. 282–308
- Katili, I., Aristio, R., 2017. Isogeometric Galerkin in Rectangular Plate Bending Problem based on UI Approach. *European Journal of Mechanics - A/Solids*, Volume 67, pp. 92–107
- Lindberg, G.M., Olson, M.D., Cowper, G.R., 1969. New Development in Finite Element Analysis of Shells. *Q. Bull. Div. Mech. Eng. and the National Aeronautical Establishment, National Research Council of Canada*, Volume 4
- Mahjudin, M., Lardeur, P., Druesne F., Katili, I., 2016. Stochastic Finite Element Analysis of Plates with the Certain Generalized Stresses Method. *Structural Safety*, Volume 61, pp. 12–21
- Maknun, I.J., Katili, I., Purnomo, H., 2015. Development of DKMT Element for Error Estimation in Composite Plate Structures. *International Journal of Technology*, Volume 6(5), pp. 780–789
- Maknun, I.J., Katili, I., Millet, O., Hamdouni, A., 2016. Application of DKMQ24 Shell Element for Twist of Thin-walled Beams: Comparison with Vlasov Theory. *International Journal for Computational Methods in Engineering Science and Mechanics*, Volume 17(5–6), pp. 391–400
- Mindlin, R.D., 1951. Influence of Rotatory Inertia and Shear on Flexural Motions of Isotropic, Elastic Plates. *Journal of Applied Mechanics*, Volume 18, pp. 31–38
- Payen, D.J., Bathe, K.J., 2011. The Use of Nodal Point Forces to Improve Element Stresses. *Computers and Structures*, Volume 89, pp. 485–495
- Payen, D.J., Bathe, K.J., 2012. A Stress Improvement Procedure. *Computers and Structures*, Volume 112–113, pp. 311–326
- Reissner, E., 1943. The Effect of Transverse Shear Deformation on the Bending of elastic Plates. *Journal of Applied Mechanics in Engineering ASME*, Volume 12, pp. A69–A77
- Scordelis, A.C., Lo, K.S., 1969. Computer Analysis of Cylindrical Shells. *Journal of American Concrete Institute*, Volume 61, pp. 539–562
- Ubertini, F., 2004. Patch Recovery based on Complimentary Energy. *International Journal for Numerical Methods in Engineering*, Volume 59, pp. 1501–1538

- Yunus, S.M., Pawlak, T.P., Wheeler, J.M., 1990. Application of the Zienkiewicz-zhu Error Estimator for Plate and Shell Analysis. *International Journal for Numerical Methods in Engineering*, Volume 29, pp. 1281–1298
- Wong, F.T., Erwin, Richard, A., Katili, I., 2017. Development of DKMQ Element for Buckling Analysis of Shear-deformable Plate Bending. *Procedia Engineering*, Volume 171, pp. 805–812
- Zhang, Z., Naga, A., 2004. Polynomial Preserving Gradient Recovery and a Posteriori Estimate for Bilinear Element on Irregular Quadrilaterals. *International Journal of Numerical Analysis and Modeling*, Volume 1(1), pp. 1–24
- Zienkiewicz, O.C., Zhu, J.Z., 1987. A Simple Error Estimator and Adaptive Procedure for Practical Engineering Analysis. *International Journal for Numerical Methods in Engineering*, Volume 24, pp. 337–357
- Zienkiewicz, O.C., Zhu, J.Z., 1989. Error Estimates and Adaptive Refinement for Plate Bending Problems. *International Journal for Numerical Methods in Engineering*, Volume 28, pp. 2839–2853
- Zienkiewicz, O.C., Zhu, J.Z., 1992a. The Superconvergent Path Recovery (SPR) and Adaptive Finite Element Refinement. *Computer Methods in Applied Mechanics and Engineering*, Volume 101, pp. 207–224
- Zienkiewicz, O.C., Zhu, J.Z., 1992b. The Superconvergence Patch Recovery and a Posteriori Error Estimation in the Finite Element Method, Part 1: The Recovery Technique. *International Journal for Numerical Methods in Engineering*, Volume 33, pp. 1331–1364
- Zienkiewicz, O.C., Zhu, J.Z., 1992c. The Superconvergence Patch Recovery and a Posteriori Error Estimation in the Finite Element Method, Part 2: Error E and Adaptivity. *International Journal for Numerical Methods in Engineering*, Volume 33, pp. 1365–1382